Title

Deregulated 14-3-3ζ and methionine adenosyltransferase α1 interplay promotes liver cancer tumorigenesis in mice and humans.

Journal

Oncogene, 40(39)

ISSN

0950-9232

Authors

Lu, Liqing
Zhang, Jing
Fan, Wei
et al.

Publication Date

2021-09-01

DOI

10.1038/s41388-021-01980-6

Peer reviewed

ARTICLE

Deregulated 14-3-3ζ and methionine adenosyltransferase α1 interplay promotes liver cancer tumorigenesis in mice and humans

Liqing Lu[1,2,8], Jing Zhang[1,3,8], Wei Fan[1,8], Yuan Li[1,4], Jiaohong Wang[1], Tony W. H. Li[1], Lucia Barbier-Torres[1], José M. Mato[5], Ting Liu[2,4], Ekihiro Seki[1], Michitaka Matsuda[1], Maria Lauda Tomasi[1], Neil A. Bhowmick[6,7], Heping Yang[1✉] and Shelly C. Lu[1✉]

Methionine adenosyltransferase 1A (MAT1A) is a tumor suppressor downregulated in hepatocellular carcinoma and cholangiocarcinoma, two of the fastest rising cancers worldwide. We compared MATα1 (protein encoded by *MAT1A*) interactome in normal versus cancerous livers by mass spectrometry to reveal interactions with 14-3-3ζ. The MATα1/14-3-3ζ complex was critical for the expression of 14-3-3ζ. Similarly, the knockdown and small molecule inhibitor for 14-3-3ζ (BV02), and ChIP analysis demonstrated the role of 14-3-3ζ in suppressing MAT1A expression. Interaction between MATα1 and 14-3-3ζ occurs directly and is enhanced by AKT2 phosphorylation of MATα1. Blocking their interaction enabled nuclear MATα1 translocation and inhibited tumorigenesis. In contrast, overexpressing 14-3-3ζ lowered nuclear MATα1 levels and promoted tumor progression. However, tumor-promoting effects of 14-3-3ζ were eliminated when liver cancer cells expressed mutant MATα1 unable to interact with 14-3-3ζ. Taken together, the reciprocal negative regulation that MATα1 and 14-3-3ζ exert is a key mechanism in liver tumorigenesis.

Oncogene (2021) 40:5866–5879; https://doi.org/10.1038/s41388-021-01980-6

INTRODUCTION

Methionine adenosyltransferase (MAT) is an essential enzyme as it is responsible for the biosynthesis of S-adenosylmethionine (SAMe), the principal methyl donor [1]. Of the two MAT genes that encode for the MAT catalytic subunits, *MAT1A* is primarily expressed in hepatocytes and bile duct epithelial cells [1, 2]. MAT1A expression falls in hepatocytes and bile duct epithelial cells during chronic cholestasis, in murine and human hepatocellular carcinoma (HCC), and cholangiocarcinoma (CCA) [2]. Lower MAT1A expression is associated with worse prognosis in HCC [3]. Downregulation of *MAT1A* expression in liver disease and HCC have been attributed to promoter and coding region hypermethylation [4, 5], histone H4 deacetylation [4], and increased interaction of *MAT1A* 3′UTR with AUrich RNA binding factor 1, which destabilize *MAT1A* mRNA [6]. We have also shown *MAT1A* transcription is inhibited by c-MYC, MAFG [7], and FOXM1 [3], transcription factors that are upregulated in liver cancers.

MATα1, the protein encoded by *MAT1A*, is present in the cytosol, nucleus and mitochondria in hepatocytes and suppresses tumorigenesis via multiple mechanisms [8]. Higher nuclear MATα1 level can lead to higher SAMe level and suppress oncogenes like *LIN-28B* via promoter hypermethylation [9]. In addition, MATα1 interacts with multiple transcription factors to regulate gene transcription as a co-repressor. MATα1 can heterodimerize with MAX to bind and repress E-box-dependent genes [10]. MATα1 also interacts with p50 and p65 to repress NF-κB-dependent reporter activity [3, 7], and NF-κB and FOXM1 to repress *FOXM1* promoter activity at the FOX binding site [3]. Thus, higher nuclear MATα1 level is key to suppressing liver cancer but regulation of nuclear MATα1 content is unknown. Here we took an unbiased approach to define its protein interactome in normal liver as compared to liver cancers. This led us to unveil a complex crosstalk between MATα1 and 14-3-3ζ that is important in both HCC and CCA.

MATERIALS AND METHODS

Please see Supplemental Methods for kinase prediction, in vitro kinase assay, promoter constructs and luciferase assays, cell lines treatments, site-directed mutagenesis, histology and immunohistochemistry, phosphoprotein enrichment and nuclear protein extraction, western blotting, immunofluorescence, RNA isolation and real-time PCR, chromatin immunoprecipitation (ChIP) and sequential ChIP, electrophoretic mobility assay, recombinant protein interaction, growth, migration and invasion assays, proteomics and mass spectrometry. Key resources are listed in Table S1.

Human samples

CCA and adjacent non-tumorous tissues are from: 1) seven patients that underwent surgical resection at Cedars-Sinai Medical Center

[1]Karsh Division of Gastroenterology and Hepatology, Cedars-Sinai Medical Center, Los Angeles, CA, USA. [2]Key Laboratory of Cancer proteomics of Chinese Ministry of Health, Xiangya Hospital, Central South University, Changsha, Hunan, China. [3]Department of Oncology, Tongji Hospital, Tongji Medical College, Huazhong University of Science and Technology, Wuhan, China. [4]Department of Gastroenterology, Xiangya Hospital, Central South University, Changsha, Hunan, China. [5]CIC bioGUNE, Centro de Investigación Biomédica en Red de Enfermedades Hepáticas y Digestivas (Ciberehd), Technology, Park of Bizkaia, Derio, Bizkaia, Spain. [6]Department of Biomedical Sciences, Cedars-Sinai Medical Center, Los Angeles, CA, USA. [7]Cancer Biology Program, Samuel Oschin Comprehensive Cancer Institute, Cedars-Sinai Medical Center, Los Angeles, CA, USA. [8]These authors contributed equally: Liqing Lu, Jing Zhang, Wei Fan. ✉email: Heping.yang@cshs.org; shelly.lu@cshs.org

Received: 29 January 2021 Revised: 14 July 2021 Accepted: 22 July 2021
Published online: 4 August 2021

A Potential MATα1 interacting proteins after Co-IP of tumorous and control lysates with anti-MATα1 antibody followed by mass spectrometry

	Protein Names	Scores
hNL	CPS1	434.21
	ATP5B	71.78
	KRT8	44.88
	MYH9	33.32
	H2AFY	30.64
	HSPA8	26.13
	MATα1	24.19

	Protein Names	Scores
hHCC	CPS1	769.08
	ATP5A1	83.89
	PCK2	72.04
	ATP5B	69.12
	14-3-3ζ	63.86
	KRT1	57.55
	EHHADH	53.22

	Protein Names	Scores
mNL	CPS1	1397.44
	MATα1	105.47
	HADHA	59.68
	ACAA2	57.81
	CLTC	57.8
	ALDH2	57.6
	IGKC	56

	Protein Names	Scores
mCCA	CPS1	1099.93
	KRT18	188.53
	BHMT	129.37
	APT5B	90.18
	14-3-3ζ	88.70
	KRT8	72.30
	IGKC	59.38

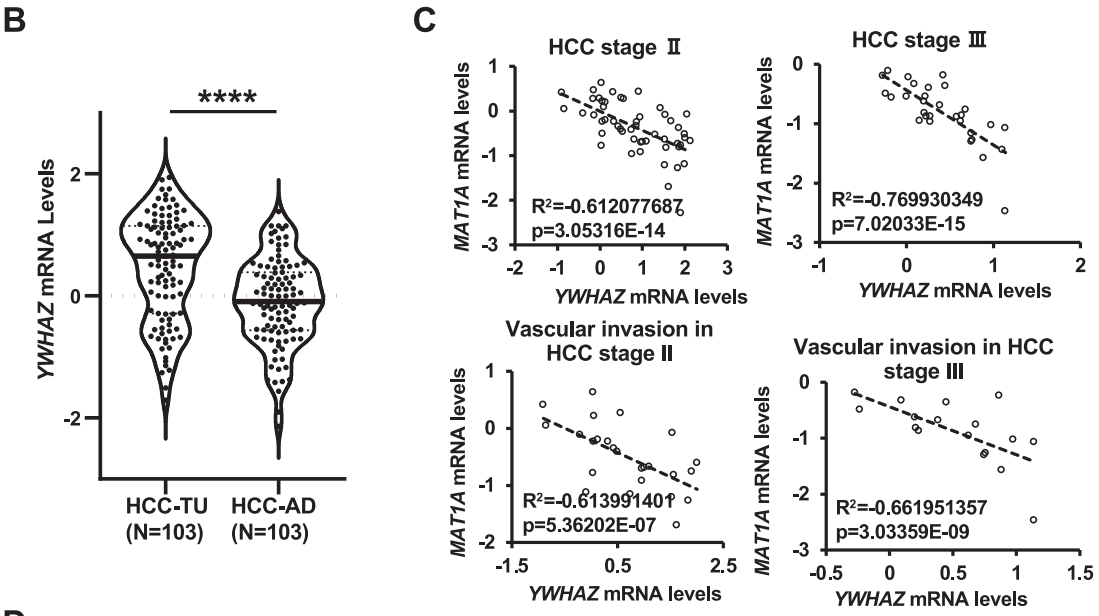

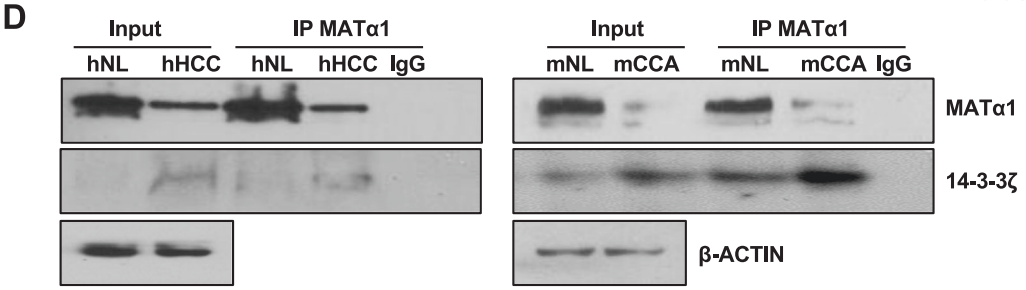

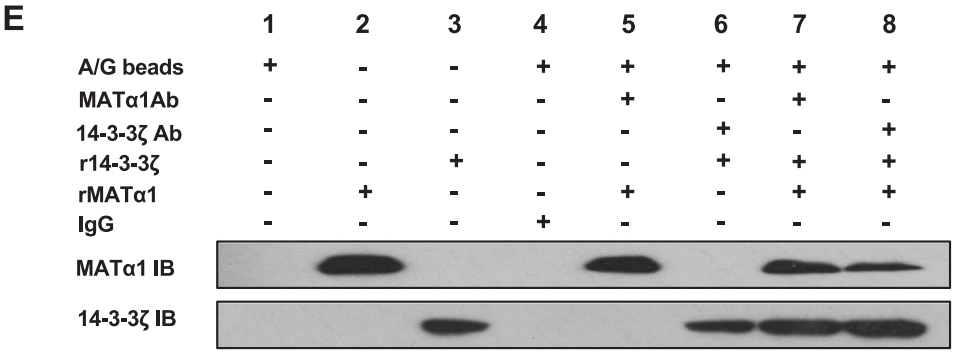

Fig. 1 Interaction between MATα1 and 14-3-3ζ and correlation between *YWHAZ* and *MAT1A* mRNA levels in HCC grades and vascular invasion. A Potential MATα1 interacting proteins after co-immunoprecipitation (Co-IP) of human normal liver (hNL), human HCC (hHCC), mouse normal liver (mNL), and mouse CCA (mCCA) lysates with anti-MATα1 antibody followed by mass spectrometry. Three specimens per group were pooled for the IP. **B** Relative mRNA levels of *YWHAZ* in HCC (HCC-TU) and adjacent non-tumorous (HCC-AD) liver tissues from 103 patients (log 10 scale). ****$P < 0.0001$ vs. HCC-AD. **C** Pearson correlation analyses between *MAT1A* and *YWHAZ* mRNA levels (log 10) in 52 HCC stage II and 30 HCC stage III patients, and in 25 HCC stage II and 17 HCC stage III patients with vascular invasion. **D** MATα1 and 14-3-3ζ interaction in hNL, hHCC, mNL, and mCCA was detected by Co-IP and western blotting. **E** In vitro pull-down shows direct interaction between MATα1 and 14-3-3ζ using recombinant MAT1α1 and 14-3-3ζ proteins. Results represent three independent experiments done in duplicate.

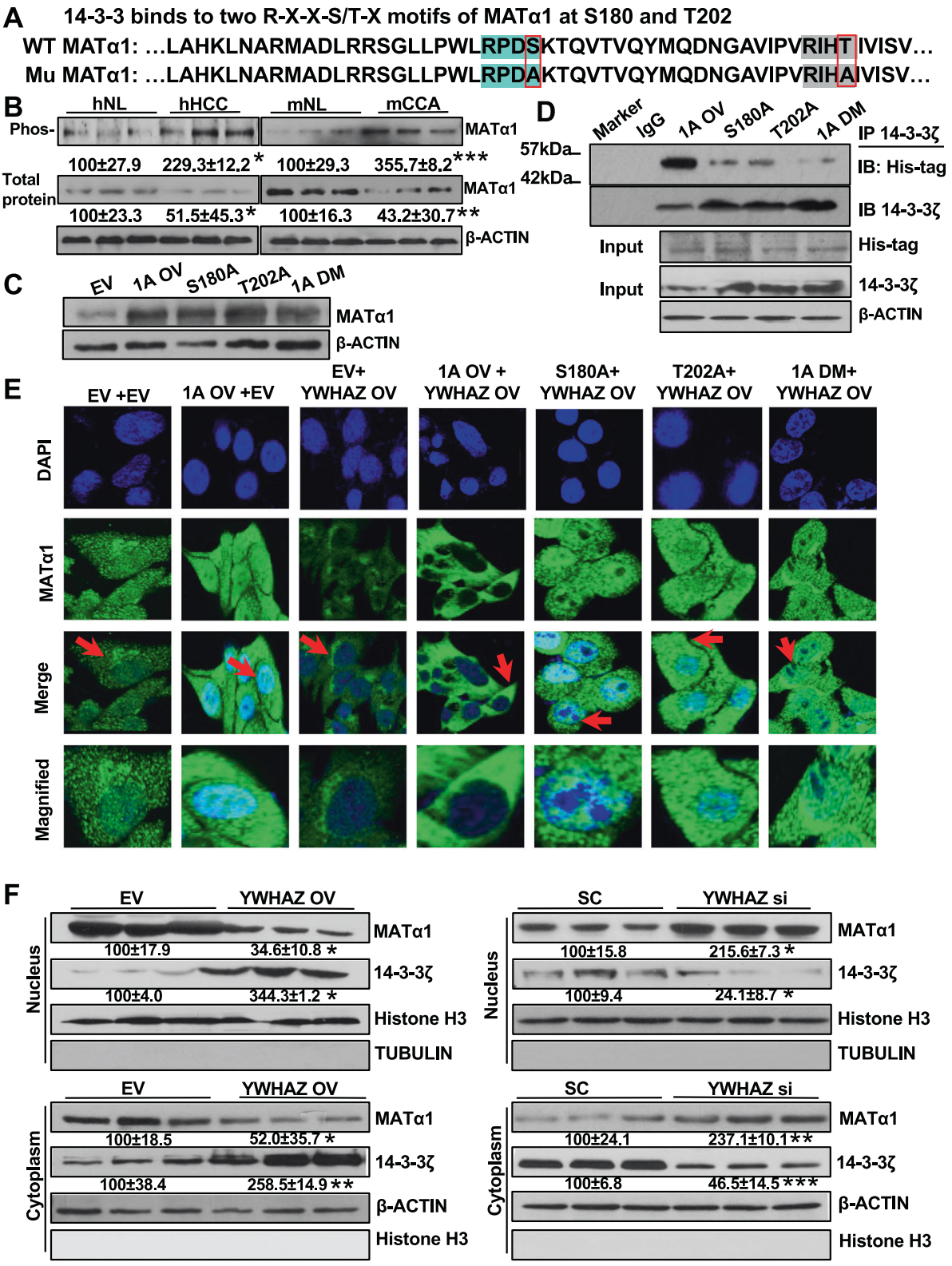

(CSMC), Los Angeles, CA, and 2) four paired tissues from the CSMC Biobank. HCC and adjacent non-tumorous tissues are from: 1) five paired tissues come from the CSMC Biobank, and 2) 103 patients that underwent surgical liver resection from 2013 to 2017 at the Xiangya Hospital Central South University, Changsha, Hunan province, China, which were stored in liquid nitrogen and transferred to the −80 °C refrigerator in the institutional biobank. All human materials were obtained with patients' informed contents. The study protocol was approved by the Institutional Review Boards of CSMC (No. 39428) and the Medical Ethical Committee of Xiangya Hospital Central South University (No. 202004246). The diagnosis in each case was determined by pathologists.

Fig. 2 Interaction between 14-3-3ζ and MATα1 requires MATα1 phosphorylation and lowers MATα1 nuclear content. A MATα1 contains two potential 14-3-3ζ binding sites at 180 S and 202 T. **B** Phosphorylated proteins were isolated as described in Methods and western blotting performed for phosphorylated and total MATα1 protein levels in hHCC, mCCA, and respective normal livers (labeled as hNL and mNL). Densitometric values are summarized below the blots, expressed as mean % of respective NLs ± SEM. *$P < 0.05$, **$P < 0.01$, ***$P < 0.001$ vs. respective NLs. **C** MATα1 protein levels after transfections of empty vector (EV), wild type MAT1A overexpression (1A OV), MAT1A S180A mutant (S180A), MAT1A T202A mutant (T202A), or MAT1A S180A and T202A double mutant (1A DM) vectors in His-tag for 24 h in HepG2 cells. **D** Immunoprecipitation (IP) of total lysates from HepG2 cells after 1A OV, S180A, T202A or 1A DM transfection for 24 h using anti-14-3-3ζ antibody or IgG, followed by immunoblotting (IB) for His-tag and 14-3-3ζ. **E** Immunofluorescence (IF) of MATα1 in HepG2 cells after transfections of EV + EV, EV + MAT1A OV, EV + YWHAZ OV, YWHAZ OV combined with 1A OV, S180A, T202A or 1A DM vectors. The top row shows DAPI staining. The second row shows the MATα1 staining. The third row merged DAPI and MATα1 staining (original magnification, x 630 (oil immersion)) and the fourth row shows magnified images of the regions indicated by red arrows. **F** Western blots show MATα1 and 14-3-3ζ protein levels after YWHAZ overexpression (YWHAZ OV) or siRNA knockdown (YWHAZ si) in nuclear and cytosolic compartments of HepG2 cells after 24 h. Densitometric values are summarized below the blots, expressed as mean % of EV or SC ± SEM from three experiments done in duplicates. *$P < 0.05$, **$P < 0.01$, ***$P < 0.001$ vs. EV or SC.

Mice

Mouse experiments were approved by the Institutional Animal Care of CSMC (No. 8850). C57BL/6mice were obtained from Jackson Laboratory (Bar Harbor, ME). In all experiments 6–12 weeks old male mice were used. Murine cholestasis-associated CCA model was previously described [11]. CCA specimens from our previous study were used for western blotting and Co-immunoprecipitation (Co-IP).

Cell lines

HepG2 (human hepatoblastoma), Hep3B (human hepatocellular carcinoma), and MzChA-1 (human biliary adenocarcinoma) were as we described [7]. HuCCT-1 (human intrahepatic cholangiocarcinoma) cells were provided by Dr. Gianfranco Alpini (Indiana University School of Medicine), MATα1-D (HCC cell line from *Mat1a* KO mouse in C57/B6 background), SAMe-D (another HCC cell line from *Mat1a* KO mouse), and OKER (HCC cell line from glycine N-methyltransferase KO mouse in C57/B6 background) cells were previously described [3] and cultured in DMEM containing 10% FBS, 1% Penicillin-Streptomycin solution.

Syngeneic tumorigenesis model and treatment with BV02

Three-month-old male C57BL/6J mice were injected with OKER cells (5×10^6) in 50 µl phosphate buffered saline (PBS) subcutaneously into both flanks. When the tumor reached 80mm^3 (mostly at day four after injection), mice were divided into two groups (8 mice per group), one received BV02 (25 mg/kg/d in 50 µl DMSO) via intratumoral injection every 2 days and the other received 50 µl DMSO. Tumor size was measured by calipers, and the tumor volume was calculated by the formula: volume = (length x width^2)/2. Experiment was terminated at day 12, tumor tissues were snap frozen and saved for further RNA and protein analysis or processed for histology and IHC.

Syngeneic metastatic HCC model

Six-week-old male C57BL/6J mice were injected with MATα1-D cell (5×10^6) stably expressing WT MAT1A, double mutant MAT1A (S180A, T202A), YWHAZ, or empty vector (EV) in 50 µl PBS into the spleen (n = 8 per group). YWAHZ-overexpressing adenovirus (Ad-GFP-mYWHAZ) or GFP control adenovirus (Ad-GFP control group) was injected into the tail vein of each mouse (1×10^9 PFU/each) at day 3. Mice were divided into six groups: EV+Ad-GFP, YWHAZ overexpression+Ad-GFP, WT MAT1A overexpression+Ad-GFP, double mutant MAT1A overexpression+Ad-GFP, WT MAT1A overexpression+Ad-GFP-mYWHAZ, double mutant MAT1A overexpression+Ad-GFP-mYWHAZ. The size of the liver tumor and metastasis were monitored by PerkinElmer IVIS® SPECTRUM system at day 7. Animals were sacrificed at day 10. Tumor tissues were processed for protein analysis, including histology.

Bioinformatics

To identify differential mRNA expression of *MAT1A* and *YWHAZ* in HCC and CCA, public genomic profile was retrieved from illumine BaseSpace Correlation Engine (https://www.illumina.com/products/by-type/informatics-products/basespace-correlation-engine.html). Graph showing survival analysis of *YWHAZ* was generated using TCGA dataset from OncoLnc (http://www.oncolnc.org/).

Quantification and statistical analysis

Data are expressed as mean ± standard error. Data were analyzed using two-tailed unpaired Student's t-test for comparing two groups and analysis of variance followed by Fisher's test for multiple comparisons. The ratios of genes or proteins expression levels to housekeeping genes or proteins were calculated. Student's t-test was used for Pearson correlation. Log-rank test was performed for survival analysis. Significant difference was defined by $p < 0.05$.

RESULTS

14-3-3ζ is a top interacting protein of MATα1 in liver cancer

To define the MATα1 interactome, we performed IP with an anti-MATα1 antibody followed by MS using liver lysates from human HCC and adjacent liver tissues, mouse CCA and normal mouse liver [11]. Of the top 150 scoring proteins, 14-3-3ζ was among the top five highest scores in human HCC and mouse CCA (Fig. 1A and Tables S2–5). We focused on 14-3-3ζ because this is the only one that exhibits increased interaction in both liver cancers and patients with high *YWHAZ* mRNA levels in HCC have shorter overall survival [12]. Consistently, *YWHAZ* mRNA levels from 103 HCC tumor tissues are significantly higher than adjacent non-tumorous tissues (Fig. 1B). High *YWHAZ* mRNA levels correlated with older age, HCC stage, but not with gender, alpha-fetoprotein (AFP) levels, vascular invasion, or tumor size (Table S6). There is an inverse relationship between *YWHAZ* and *MAT1A* mRNA levels especially in the more advanced HCC stages and those with vascular invasion (Fig. 1C), and in the TCGA HCC datasets (Fig. S1A), which show patients with higher *YWHAZ* mRNA levels had lower survival (Fig. S1B).

To confirm our MS results, we performed Co-IP with human HCC, mouse CCA and normal human or mouse liver lysates and found despite lower levels of MATα1 in the cancer tissues, interaction with 14-3-3ζ is higher (Fig. 1D). We next used recombinant MATα1, 14-3-3ζ, and specific antibodies immobilized to A/G beads and found MATα1 and 14-3-3ζ can interact directly (Fig. 1E).

Interaction between 14-3-3ζ and MATα1 requires phosphorylation of MATα1 at S180 and T202, results in nuclear exclusion of MATα1

MATα1 contains two canonical RXX(S/T)XP motifs [13] at S180 and T202 (Fig. 2A). Despite a 50% drop in total MATα1 level, phospho-MATα1 levels were 2 to 3-fold higher in human HCC and mouse CCA (Fig. 2B). We then mutated S180 and T202 to alanine and wild type (WT), S180A, T202A, or double mutants in His tags were overexpressed in HepG2 cells (Fig. 2C). Interaction between 14-3-3ζ and MATα1 was reduced in the S180A and T202A mutants and nearly eliminated with the double mutant (Fig. 2D).

We next examined whether 14-3-3ζ can influence MATα1 subcellular localization. In HepG2 cells, overexpressing MAT1A raised cytoplasmic and nuclear MATα1 content, whereas overexpressing YWHAZ lowered both on immunofluorescent (IF) staining (Fig. 2E). When both YWHAZ and WT MAT1A were overexpressed, there is a dramatic reduction in nuclear MATα1 content compared to WT MAT1A overexpression (1A+EV). However, S180A and T202A single mutants of MAT1A had more

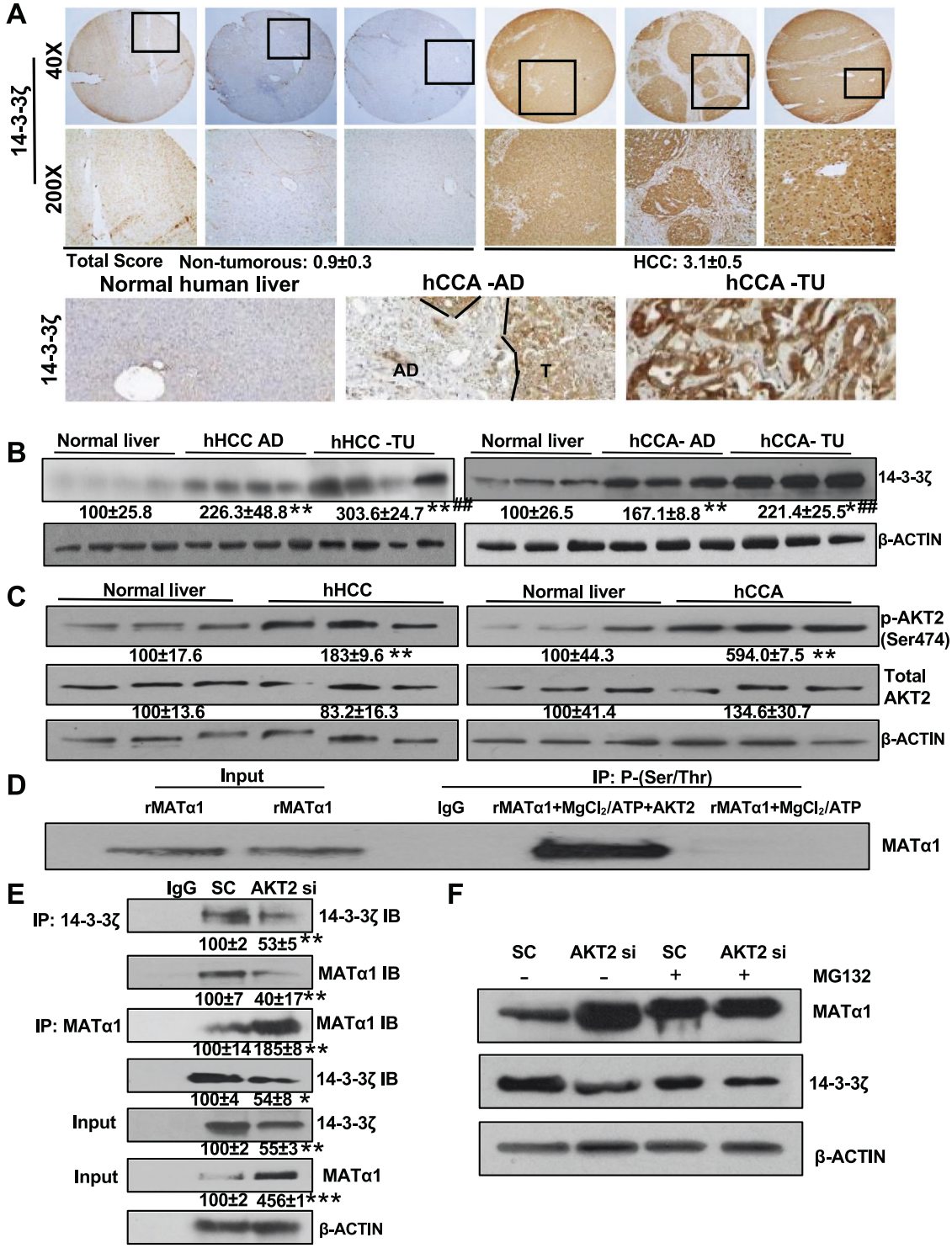

nuclear MATα1 and the double mutant of MAT1A had the most nuclear MATα1 when co-overexpressed with YWHAZ as compared to WT MAT1A+YWHAZ overexpression (Fig. 2E). The same findings were observed in Hep3B cells as well (Fig. S1C). Western blotting of nuclear and cytoplasmic compartments confirmed overexpressing YWHAZ lowered nuclear MATα1 level while knocking down YWHAZ raised it (Fig. 2F). However, cytosolic MATα1 content was also lower upon YWHAZ overexpression (Fig. 2E, F), suggesting in addition to interacting with MATα1, 14-3-3ζ also regulates MATα1's expression negatively.

Fig. 3 14-3-3ζ and AKT2 expression in liver cancers, the effects of AKT2 on MATα1 phosphorylation and interaction with 14-3-3ζ. A Top panel: Representative immunohistochemistry (IHC) staining of 14-3-3ζ in sixteen non-tumorous and HCC tumors. Images are 40X for the top row and 200X for the bottom row. Total score was calculated as described [26, 32] and summarized below the bottom row. Bottom panel: Representative IHC staining of 14-3-3ζ from 4 each of normal human liver, CCA adjacent and CCA tumor tissues (200X). **B** Total 14-3-3ζ levels in 4 normal human liver and 4 pairs of HCC and adjacent non-tumorous tissues (HCC-AD) (left panel); 3 normal human livers and 3 pairs of CAA and adjacent non-tumorous tissues (CCA AD) (right panel) were measured using western blotting. Densitometric values are summarized below of the blots, expressed as mean% of normal liver ± SEM. $^{*}P < 0.05$, $^{**}P < 0.01$ vs. normal liver, $^{\#\#}P < 0.01$ vs. adjacent liver tissues. **C** Total and phospho-AKT2 (Ser474) protein levels from normal human liver, HCC (hHCC), and CCA (hCCA) were measured by western blotting. Densitometric values are summarized below the blots, expressed as mean% of normal liver ± SEM. $^{*}P < 0.05$, $^{**}P < 0.01$ vs. normal liver. **D** AKT2 phosphorylates MATα1 in in vitro kinase assay. **E** Effect of AKT2 knockdown on interaction between 14-3-3ζ and MAT1α1 was examined by Co-IP followed by immunoblotting (IB) after treating HepG2 cells with scramble (SC) or AKT2 siRNA (AKT2 si) for 24 h. Densitometric values are summarized below the blots, expressed as mean% of SC ± SEM from three independent experiments. $^{*}P < 0.05$, $^{**}P < 0.01$, $^{***}P < 0.001$ vs. SC. **F** Western blot analysis of MAT1α1 and 14-3-3ζ in HepG2 cells were treated with scramble (SC) or AKT2 siRNA (AKT2 si) for 42 h before the addition of MG132 (20 μM) for 6 h.

We reported MATα1 level is lower in HCC and CCA [2, 9]. Here we found the opposite for 14-3-3ζ levels (Fig. 3A, B). Furthermore, 14-3-3ζ levels are already elevated in the adjacent non-tumorous tissues (Fig. 3B). Expression of 14-3-3ζ is also much higher in *Mat1a* knockout (KO) HCC than in WT mice liver tissue (Fig. S2A).

AKT2 mediates MATα1 phosphorylation and interaction with 14-3-3ζ

AKT kinases are predicted to phosphorylate both S180 and T202 of MATα1 and AKT2 has the highest score for MATα1 T202 (Fig. S2B). We focused on AKT2 because phospho-AKT2 (Ser474) levels are higher in HCC and CCA, while the total levels of AKT1, AKT2, AKT3 and phospho-AKT1 and phospho-AKT3 are unchanged (Figs. 3C, S2C). In vitro kinase assay confirmed that AKT2 is able to phosphorylate MATα1 (Fig. 3D). Silencing AKT2 reduced the interaction between MATα1 and 14-3-3ζ (Fig. 3E). Interestingly, AKT2 knockdown raised MATα1 and lowered 14-3-3ζ levels (Fig. 3E) while their mRNA levels were unchanged (data not shown). One possible mechanism is that AKT2-mediated phosphorylation of MATα1 increased MATα1 degradation. However, we found no difference in protein stability of WT MATα1 and MATα1 double mutant (Fig. S2D). Another possible mechanism is reduced proteasomal degradation. Indeed, treatment with the proteasome inhibitor MG132 raised MATα1 level and AKT2 silencing no longer had any effect (Fig. 3F).

Reciprocal regulation between YWHAZ and MAT1A

To examine reciprocal regulation between YWHAZ and MAT1A we varied their expression and found they negatively regulate each other's expression in HepG2, Hep3B, HuCCT-1, and MzChA-1 cells (Figs. 4A–D and S3A–D). However, compared to WT MAT1A, the catalytic mutant of MAT1A failed to inhibit YWHAZ expression (Fig. 4E). Inhibiting DNA methylation with 5-aza-2′-deoxycytidine (5-aza) raised *YWHAZ* mRNA levels but did not prevent MAT1A overexpression from lowering *YWHAZ* mRNA levels (Fig. S3E). Inhibiting Enhancer of Zeste Homolog 2, a histone-lysine N-methyltransferase that is primarily involved in methylating histone 3 lysine 27 (H3K27) leading to transcriptional repression [2], also raised *YWHAZ* mRNA levels but did not prevent MAT1A over-expression from lowering *YWHAZ* mRNA levels (Fig. S3F). Lastly, GEO databases verified that increased *YWHAZ* and decreased *MAT1A* mRNA levels occur in HCC of different stages, grades, etiologies, and CCA (Table S7).

14-3-3ζ regulates MAT1A transcription negatively via multiple repressor elements

YWHAZ knockdown raised the reporter activity driven by the *MAT1A* −839/+1 promoter construct maximally suggesting important elements are within this region (Fig. 5A). There are multiple binding sites of FOX and C/EBP, as well as E-box, HFH-2, GRE, NF-κB, and HNF-4 in this region (Figs. 5B and S4A, B). EMSA assay after YWHAZ siRNA treatment showed decreased protein binding to the FOX, E-box, and C/EBP elements, but the C/EBP (−683 to −695), HFH-2, GRE, NF-κB, and HNF-4 elements were unchanged (Figs. 5B and S4C, D). Mutation at each of the FOX binding sites, E-box, or C/EBP (−455 to −461) raised *MAT1A* promoter activity by about 50% but mutating all of these sites raised it by more than 3.5-fold (Fig. 5C, left graph). YWHAZ knockdown increased *MAT1A* promoter activity, but this was attenuated with each individual mutation and completely eliminated when all elements were mutated (Fig. 5C, right graph). ChIP assay showed YWHAZ knockdown lowered FOXM1, c-MYC, and C/EBPβ binding to respective regions of the *MAT1A* promoter (Fig. 5D). These results were confirmed using quantitative PCR (Fig. S5A–C).

BV02 is a small molecule that binds to the amphipathic groove of 14-3-3ζ (Fig. S6A, B) to inhibit its binding to other proteins [14]. Interestingly, we found BV02 (5 μM for 24 h) also increased *MAT1A* promoter activity (Fig. 5A), lowered protein binding to the FOX, C/EBP, and E-box elements on EMSA (Fig. 5B) and ChIP (Figs. 5D, S5A–C). This prompted us to examine whether 14-3-3ζ might also bind to these elements. We found that although 14-3-3ζ was unable to bind directly to the FOX, C/EBP or E-box regions of the *MAT1A* promoter (no signal on ChIP), it was able to bind on Seq-ChIP and BV02 treatment lowered its binding, as well as the binding of FOXM1, c-MYC, and C/EBPβ (Figs. 5D, S5A–C). 14-3-3ζ also regulates their expression, as YWHAZ overexpression raised C/EBPβ isoforms, especially C/EBPβ LIP and FOXM1, while YWHAZ knockdown lowered them (Fig. 5E). Lastly, we found 14-3-3ζ interacts directly with FOXM1, C/EBPβ, and c-MYC (Fig. 5F). These results suggest 14-3-3ζ regulates *MAT1A* expression at the promoter level by interacting and enhancing FOXM1, c-MYC, and C/EBPβ binding to their respective elements, which are all repressors for *MAT1A* transcription.

MATα1 acts as a co-repressor to regulate YWHAZ transcription at MARE and E-box elements

MAT1A knockdown raised the reporter activity driven by the *YWHAZ* −756/+1 promoter construct maximally (Fig. 6A). Within this region are two Maf recognition elements (MAREs) and an E-box (Figs. 6A, B and S7A). MAFG is one of the small Maf proteins that can bind to both MARE and E-box. We varied the expression levels of c-MYC and MAFG and found they positively regulate YWHAZ expression (Fig. 6C). Consistently, there is a positive correlation between *YWHAZ* and *MAFG* or *c-MYC* mRNA levels in the TCGA datasets (Fig. S7B, C). We also excluded involvement of other *cis*-acting elements of the *YWHAZ* promoter by performing EMSA covering other regions (Fig. S7E).

YWHAZ promoter mutants of MARE and E-box binding sites have lower promoter activity at baseline (Fig. 6D, left graph), suggesting they are required for basal expression, and silencing

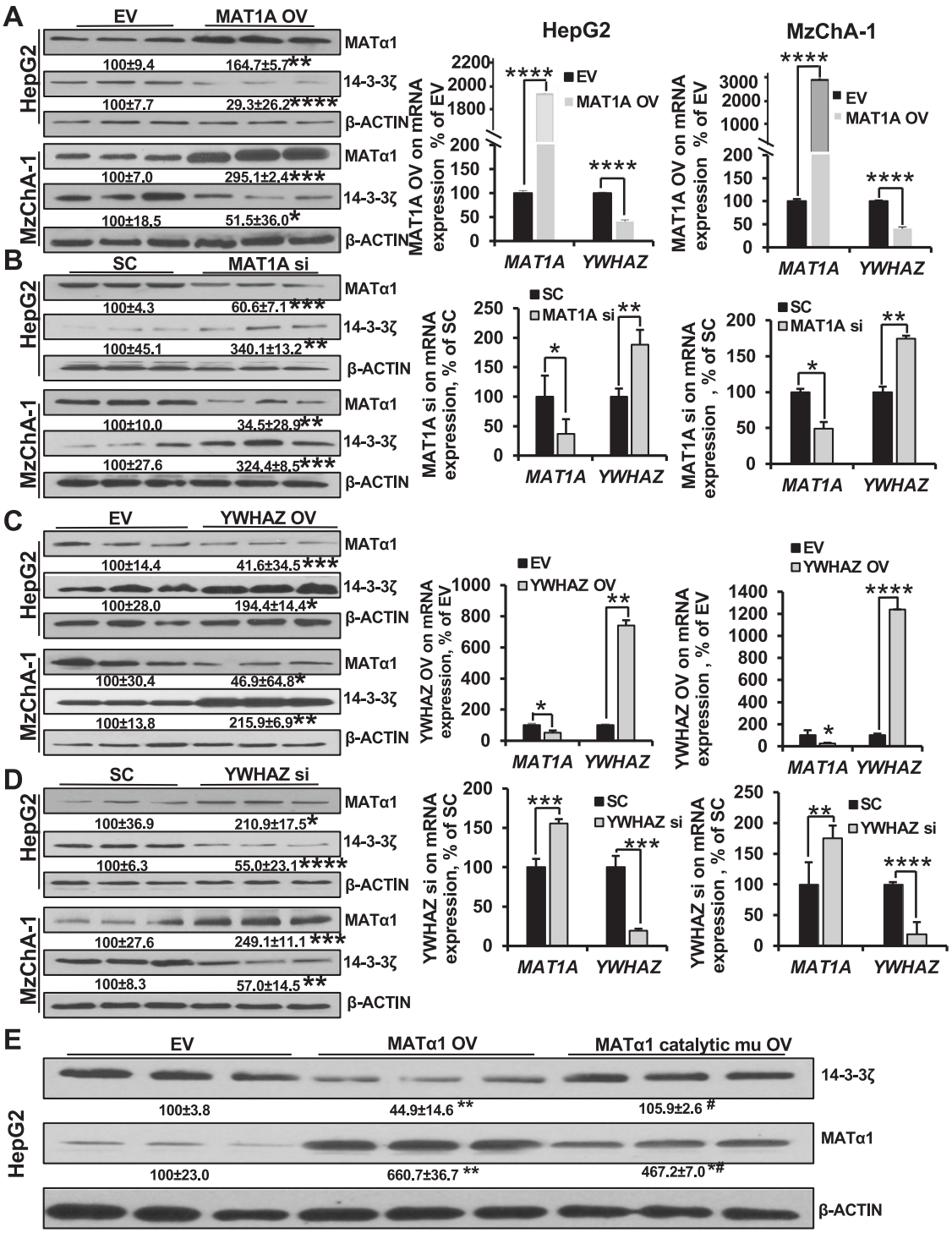

Fig. 4 Reciprocal regulation between YWHAZ and MAT1A. Protein (left panels) and mRNA levels (right panels) of MAT1A and YWHAZ from HepG2 and MzChA-1 cells after MAT1A overexpression (MAT1A OV) (**A**) or siRNA knockdown (MAT1A si) (**B**), YWHAZ overexpression (YWHAZ OV) (**C**) or siRNA knockdown (YWHAZ si) (**D**). Densitometric values are summarized below the blots, expressed as mean% EV or SC ± SEM from three experiments done in duplicates. *$P < 0.05$, **$P < 0.01$, ***$P < 0.001$, ****$P < 0.0001$ vs. EV or SC. **E** Protein levels of MATα1 and 14-3-3ζ after overexpressing wild type MAT1A (MAT1A OV), or catalytic mutant of MAT1A (MAT1A catalytic Mu OV) compared to empty vector (EV) in HepG2 cells. Densitometric values are shown below the blots, expressed as mean% of EV ± SEM, *$P < 0.05$, **$P < 0.01$, ***$P < 0.001$ vs. EV, $^{\#}P < 0.05$ vs. MAT1A OV.

MAT1A increased the WT *YWHAZ* promoter activity by 2-fold but less with mutant constructs (Fig. 6D, right graph). Importantly, MAT1A no longer exerted any effect on the *YWHAZ* promoter when MARE and E-box elements were mutated.

Only MAFG can directly bind to the MARE element by itself on ChIP. However, in the presence of MAFG, MATα1 and c-MYC co-occupied this region on Seq-ChIP (Fig. 6E). Moreover, MAT1A overexpression decreased MAFG and c-MYC binding but increased

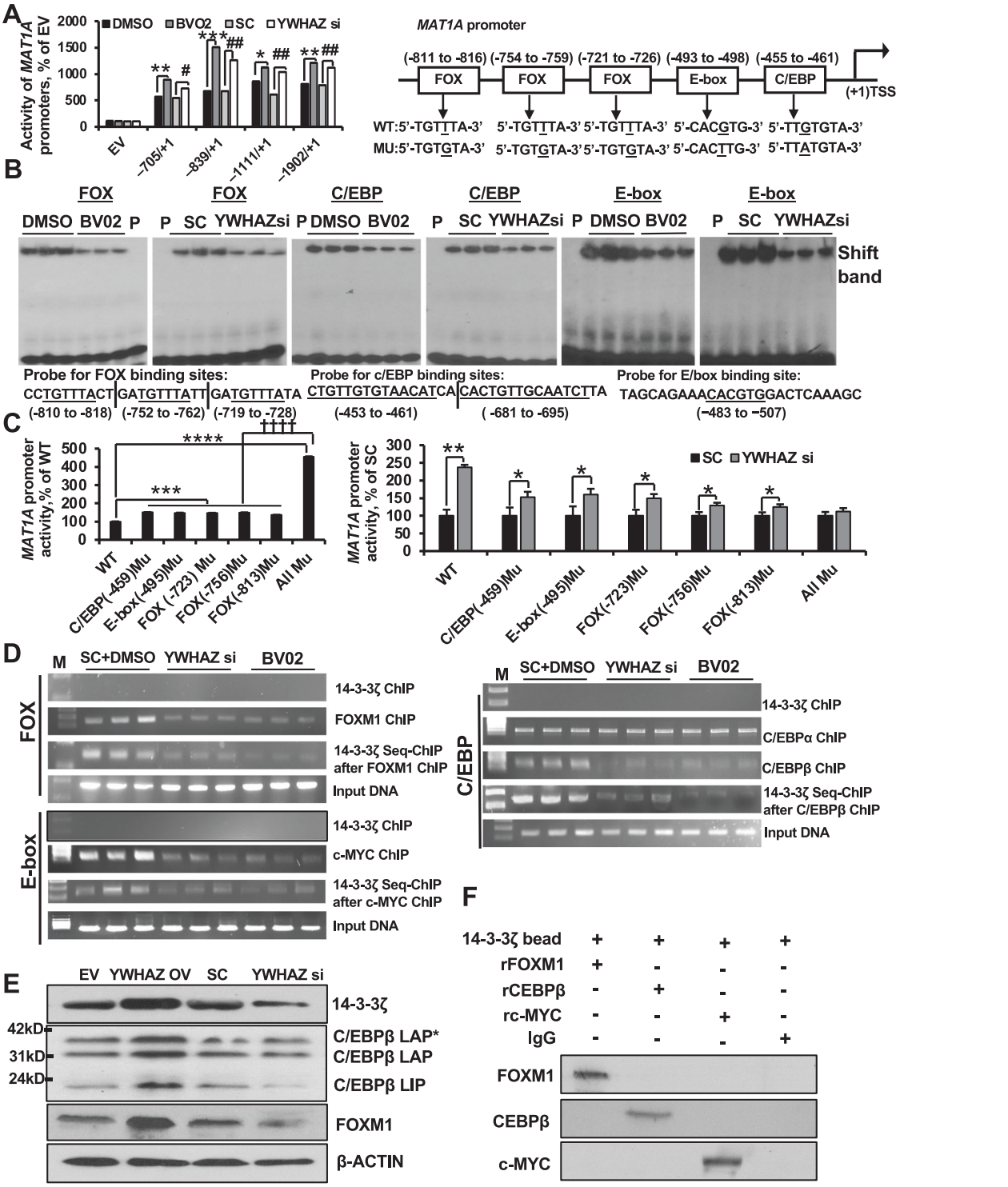

Fig. 5 Effects of YWHAZ and BV02 on the *MAT1A* promoter. A Effects of YWHAZ knockdown and BV02 (5 μM) on the *MAT1A* promoter activity in HepG2 cells. Results are expressed as mean% of EV ± SEM, $^{*}P < 0.05$, $^{**}P < 0.01$, $^{***}P < 0.001$ vs. DMSO, $^{\#}P < 0.05$, $^{\#\#}P < 0.001$. On right shows binding sites of FOX, E-box and C/EBP and their mutants in the human *MAT1A* promoter. **B** EMSA analyses using labeled probes containing three FOX elements, E-box, or C/EBP elements of the *MAT1A* promoter were performed in HepG2 cells after DMSO, BV02 (5uM), SC, or YWHAZ si treatment 24 h. Probe (P) only served as negative controls. **C** *MAT1A* promoter activities in HepG2 cells after transfection with the wild type *MAT1A* promoter (MAT1A WT), or mutated at the C/EBP element (C/EBP-459 Mu), the E-box element (E-box −495 Mu), the FOX element sites (FOX −723 Mu, FOX −756 Mu, and FOX −813 Mu), or all elements (All Mu). Left panel shows basal activity of wild type and mutant *MAT1A* promoters, right panel shows effects of YWHAZ siRNA treatment for 24 h on these same constructs. Results are expressed as mean% of WT or SC ± SEM from three experiments done in duplicates, $^{*}P < 0.05$, $^{**}P < 0.01$, $^{***}P < 0.001$, $^{****}P < 0.0001$ vs. WT or SC, $^{\dagger\dagger\dagger\dagger}P < 0.0001$ vs. all of the other constructs. **D** ChIP and Seq-ChIP analysis was performed by spanning three FOX regions, E-box regions, or C/EBP regions of the *MAT1A* promoter in HepG2 cells using 14-3-3ζ, FOXM1, c-MYC or C/EBPβ antibodies. There is no signal using anti-14-3-3ζ antibody on ChIP but there is a clear band on Seq-ChIP following FOXM1, c-MYC, or C/EBPβ ChIPs. Representative results from three experiments are shown. **E** 14-3-3ζ positively regulates C/EBPβ isoforms and FOXM1 expression. **F** 14-3-3ζ interacts with FOXM1, c-MYC, and C/EBPβ directly.

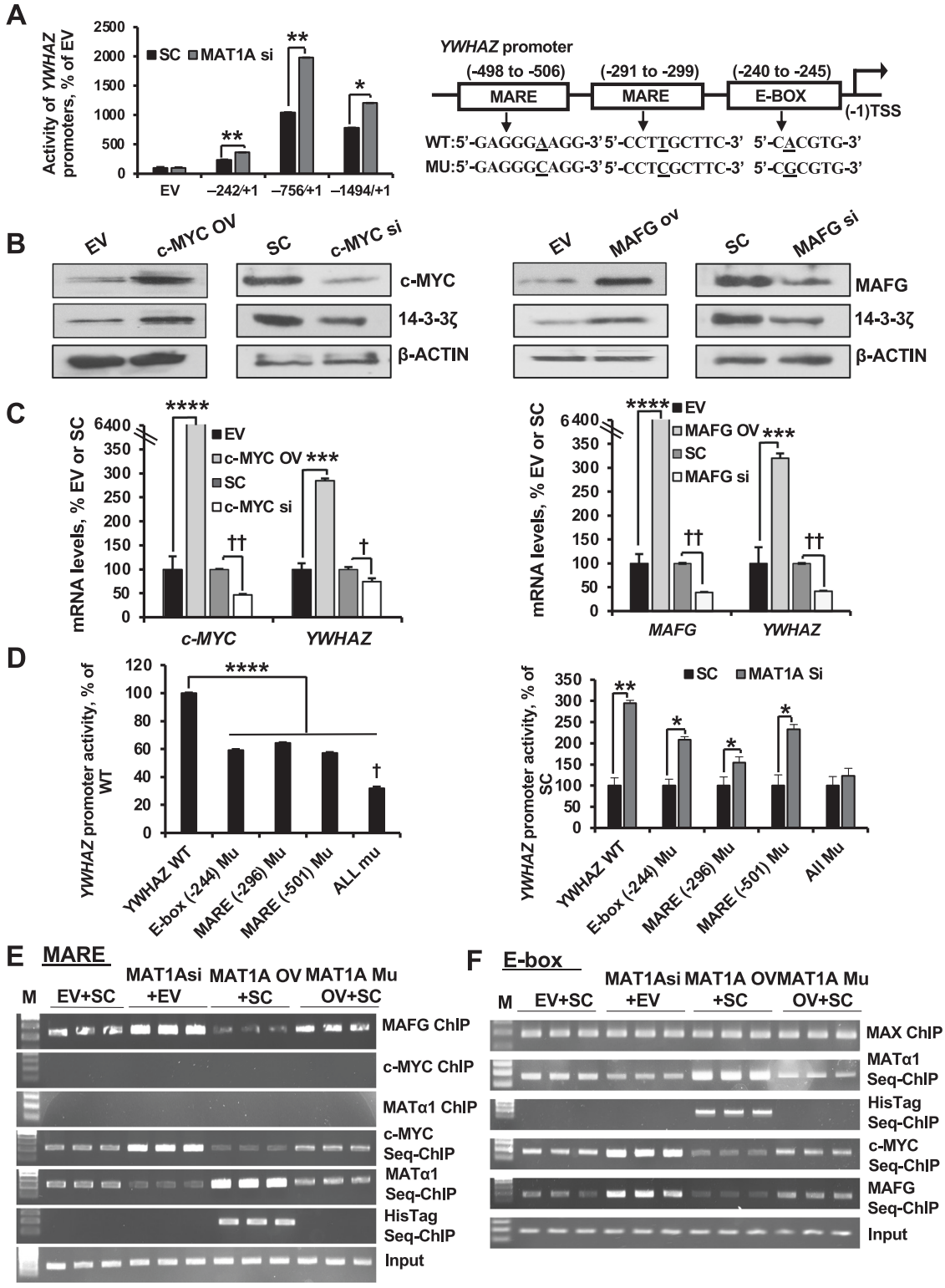

that of MATα1, and MAT1A knockdown had the opposite effects (Fig. 6E). For the E-box element, MAFG, MATα1 and c-MYC required MAX for binding to this region (Fig. 6F). MAT1A overexpression also lowered MAFG and c-MYC binding but raised that of MATα1, while silencing MAT1A had the opposite effects (Fig. 6F). These results were confirmed using quantitative PCR (Fig. S8A, B). Interestingly, the catalytic mutant of MATα1 was unable to interact with these transcription factors in binding to the promoter region of *YWHAZ* (Figs. 6E, F and S8A, B, indicated by His-tag Seq-ChIP).

Interaction between 14-3-3ζ and MATα1 is important for 14-3-3ζ to promote liver cancer cell growth, migration, and invasion

BV02 exerted a dose-dependent inhibition on the interaction between MATα1 and 14-3-3ζ (Fig. 7A) and increased MAT1A

Fig. 6 Effects of MAT1A, c-MYC and MAFG on the *YWHAZ* promoter. A MAT1A knockdown raised *YWHAZ* promoter activity in HepG2 cells. Results are mean% of EV ± SEM from three experiments done in duplicates, $^{*}P < 0.05$, $^{**}P < 0.01$ vs. SC. To the right shows MARE and E-box elements and their mutants in the human *YWHAZ* promoter. **B** c-MYC and 14-3-3ζ protein levels after c-MYC overexpression (OV) or siRNA (si) knockdown (left panel), or MAFG and 14-3-3ζ protein levels after MAFG overexpression or siRNA knockdown for 24 h in HepG2 cells (right panel). **C** *c-MYC* and *YWHAZ* mRNA levels after c-MYC OV or siRNA treatment (left panel), or *MAFG* and *YWHAZ* mRNA levels after MAFG OV or siRNA treatment in HepG2 cells (right panel). Results are mean % ± SEM of EV or SC from three experiments done in duplicates. $^{***}P < 0.001$, $^{****}P < 0.0001$ vs. EV, $^{\dagger}P < 0.05$, $^{\dagger\dagger}P < 0.01$ vs. SC. **D** Promoter activity in HepG2 cells after transfection with the wild type *YWHAZ* promoter (YWHAZ WT) and *YWHAZ* promoter mutated at various elements alone or combined (All Mu). Left panel shows basal activity of wild type and mutant *YWHAZ* promoters, right panel shows effects of MAT1A siRNA treatment for 24 h. Results are mean% of WT or SC ± SEM from three experiments done in duplicates, $^{*}P < 0.05$, $^{**}P < 0.01$, $^{****}P < 0.0001$ vs. WT or SC, $^{\dagger}P < 0.05$ vs. other mutant constructs. **E** HepG2 cells were co-transfection with MAT1A si + EV or MAT1A OV + SC, or EV + SC controls for 24 h. ChIP analysis spanning the MARE elements of human *YWHAZ* promoter was done using antibody against MAFG, c-MYC, or MATα1, and Seq-ChIP was done using antibodies to c-MYC, MATα1, or His-tag (for MATα1 catalytic mutant in His-tag) after MAFG ChIP. **F** Following the same treatments as in (**E**) ChIP analysis of the E-box binding site was performed with MAX antibody, followed by Seq-ChIP using antibodies to MATα1, c-MYC, MAFG, or His-tag for MATα1 catalytic mutant.

protein and mRNA levels (Fig. 7A, B). BV02 treatment dose-dependently suppressed OKER (HCC cell line from Glycine N-Methyltransferase knockout mouse that expresses MATα1) cell growth, migration and invasion but it had no effect on SAMe-D cells (HCC cell line from *Mat1a* KO mouse) (Fig. 7C–E). Since SAMe-D cells grow much slower than OKER cells we also examined MATα1-D (HCC cell line from another *Mat1a* KO mouse that grows much faster) [3]. BV02 still had no effect on growth, migration, or invasion in MATα1-D cells (Fig. 7C–E). Compared to primary mouse hepatocytes, OKER, SAMe-D and MATα1-D cells have much higher expression of 14-3-3ζ (Fig. S9A). We also found silencing *Ywhaz* suprpressed OKER cell growth, migration and invasion but had no effect on SAMe-D and MATα1-D cells (Fig. 7F–H). These results suggest that BV02's anti-cancer effect is mediated in a large part via MAT1A in these cell lines. To test this hypothesis we overexpressed MAT1A in SAMe-D and MATα1-D cells first before treating with BV02 and found BV02 was able to exert an inhibitory effect on growth, migration and invasion (Fig. S9B–D). We confirmed that BV02 treatment inhibited OKER cell growth in vivo using a syngeneic model and increased MAT1A expression in the tumor (Fig. S9E–H).

Since BV02 is not a specific inhibitor of 14-3-3ζ and raises MAT1A expression, we took another approach to examine the role of 14-3-3ζ and MATα1 interaction on the oncogenic properties of 14-3-3ζ in liver cancer. We compared overexpressing WT MAT1A, double mutant MAT1A (S180A and T202A), YWHAZ, alone or in combination and measured liver cancer cell growth, migration, and invasion in vitro and in vivo. Overexpressing either WT MAT1A or double mutant MAT1A lowered 14-3-3ζ, c-MYC and MAFG expression, whereas overexpressing YWHAZ had the opposite effects (Fig. 8A). Combining WT MAT1A with YWHAZ resulted in c-MYC and MAFG levels comparable to EV+EV controls. However, combining double mutant MAT1A and YWHAZ lowered c-MYC and MAFG levels, suggesting the double mutant MAT1A was able to gain nuclear entry and exert its inhibitory effect on c-MYC and MAFG expression (Fig. 8A). Effects of these treatments on migration and invasion were similar––WT and double mutant MAT1A exerted comparable inhibitory effects; YWHAZ over-expression increased all parameters but co-expression with WT MAT1A attenuated the increase, whereas co-expression with the double mutant MAT1A completely eliminated the increase (Fig. 8B, C). Finally, we examined the importance of 14-3-3ζ and MATα1 interaction using a syngeneic metastatic HCC model. The mouse and human MATα1 share high sequence homology at the two 14-3-3ζ binding sites (Fig. S10A). Importantly, the murine double mutant MAT1A was able to block YWHAZ overexpression's inductive effect on tumor growth (Figs. 8D and S10B–D) and metastasis to the pancreas much more effectively than WT MAT1A (Fig. S10E). In addition, c-MYC and MAFG levels were lower in tumors that overexpress double mutant MAT1A and YWHAZ as compared to tumors that overexpress WT MAT1A and YWHAZ (Fig. 8E).

DISCUSSION

MAT1A encodes for MATα1, which forms dimer (MATIII) and tetramer (MATI) that are mainly expressed in normal hepatocytes and cholangiocytes [1, 2]. We and others have shown MATα1 can target the nucleus where it regulates gene expression by epigenetic mechanisms [9, 15, 16], and the mitochondria where it regulates mitochondrial function [17]. MAT1A expression is often downregulated in HCC and CCA [1–3] and low MAT1A expression is associated with worse survival in HCC [18]. MATα1 can target the nucleus where it exists as tetramers and monomers, which is catalytically inactive [9, 15]. Higher nuclear MATα1 content correlated with higher levels of H3K27 trimethylation, an epigenetic mark that is associated with gene repression and DNA methylation [9, 15]. Indeed, overexpressing MAT1A resulted in higher levels of H3K27me3, hypermethylation of *LIN28B* promoter and lower LIN28B expression [9]. However, we found MATα1 can interact with many transcription factors, including MAX, c-MYC, MAFG, p50, p65, FOXM1, and serve as a co-repressor for the E-box, NF-κB, and FOX elements [2, 3, 10]. These accumulating results support the notion that nuclear MATα1 can also repress oncogenes as a transcription co-factor. Clearly higher nuclear MATα1 content is important for it to exert its tumor suppressive effects. However, what regulates MATα1 nuclear content has remained largely unknown.

In order to better understand MATα1's tumor suppressive actions we took an unbiased approach and compared its interactome in normal liver versus HCC and CCA. We used a murine CCA model due to limited human CCA tissue availability and the fact that many of the altered signaling pathways in human CCA also occurred in this model [11]. Interestingly, 14-3-3ζ emerged as an interacting protein prominently in human HCC and murine CCA. The majority of 14-3-3ζ ligands include one of the three consensus binding motifs (RXX(pS/pT)XP, RXXX(pS/pT)XP, and (pS/pT)X1-2-COOH) [19, 20]. 14-3-3 binding can regulate substrates subcellular localization [21]. MATα1 sequence contains two consensus motifs. Indeed, we found 14-3-3ζ interacts directly with MATα1 and their interaction is higher in human HCC and murine CCA. Most importantly, the interaction between 14-3-3ζ and MATα1 keeps MATα1 out of the nucleus, as demonstrated by mutating S180 and T202, two 14-3-3ζ interacting sites on MATα1. Consistently, co-overexpressing the MATα1 double mutant with 14-3-3ζ lowered c-MYC and MAFG expression as compared to co-overexpressing the wild type MATα1 with 14-3-3ζ, since the double mutant MATα1 was able to target the nucleus and repress these genes. These results are also consistent with a report that showed YWHAZ knockdown decreased nuclear p65 level in HCC-LM3 cell line [22], since higher nuclear MATα1 suppresses p65 expression [3]. This may be the first reported mechanism operative in liver cancer that keeps MATα1 out of the nucleus.

One protein that deserves mention is Carbamoyl Phosphate Synthetase 1 (CPS1), the top MATα1-interacting protein in both normal and cancerous livers. CPS1 is a mitochondrial enzyme

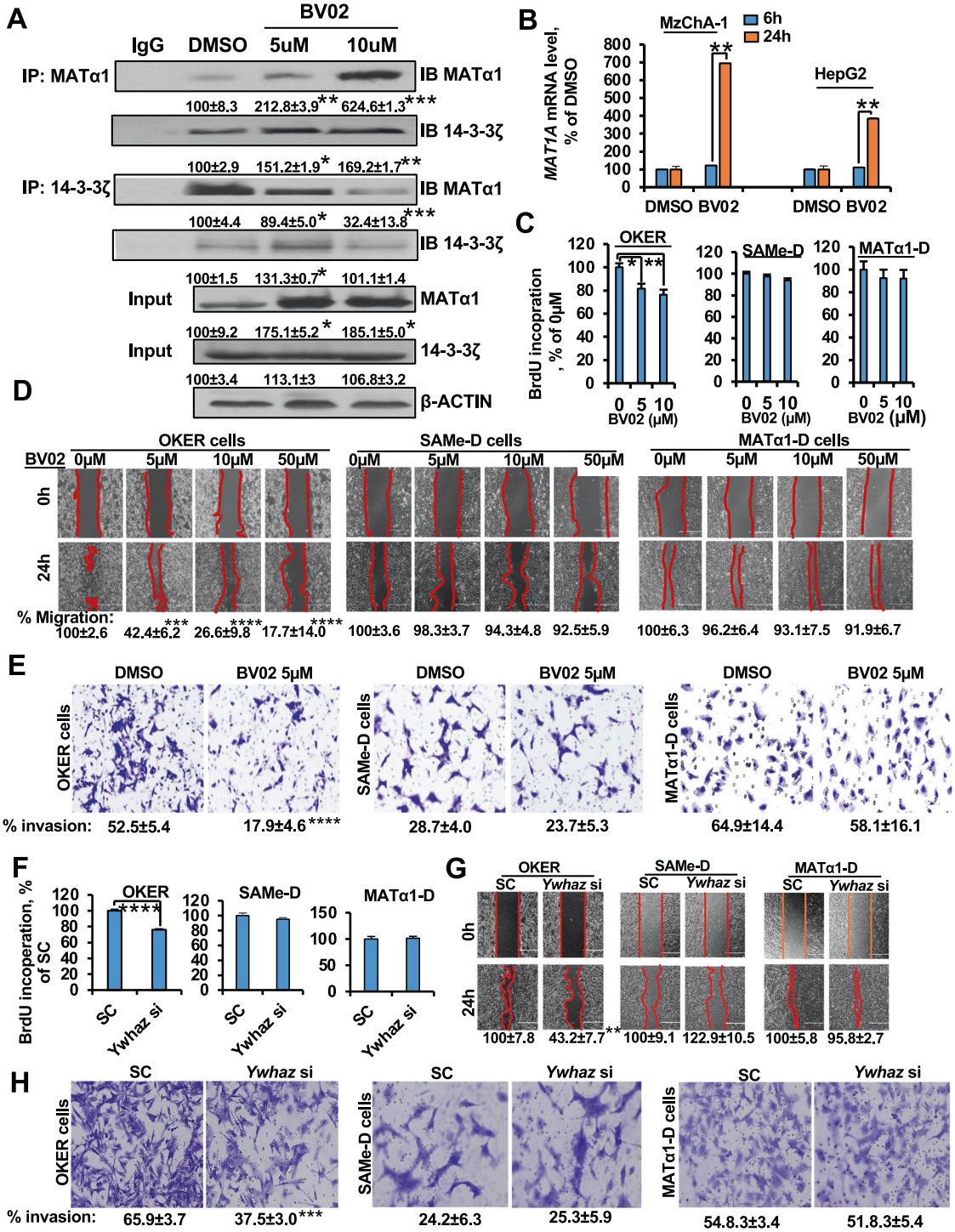

Fig. 7 Effects of BV02 on the interaction between MATα1 and 14-3-3ζ, and on growth, migration, and invasion of OKER, SAMe-D, and MATα1-D cells. A Immunoprecipitation (IP) of total lysates from HepG2 cells after BV02 treatments for 24 h with anti-MATα1 or anti-14-3-3ζ antibody, followed by Immunoblot (IB) analysis for MATα1 and 14-3-3ζ. Interaction between MATα1 and 14-3-3ζ was determined by normalizing to total levels of MATα1 and 14-3-3ζ that had been normalized to actin, $^{*}P < 0.05$, $^{**}P < 0.01$, $^{***}P < 0.001$ vs. DMSO. **B** qRT-PCR analysis of *MAT1A* mRNA levels after BV02 treatment (5 μM) for six and 24 h in MzChA-1 and HepG2 cells. Results are expressed as mean% of DMSO ± SEM from three experiments done in duplicates, $^{**}P < 0.01$ vs. DMSO. **C** BrdU assay after varying concentrations of BV02 treatment in OKER, SAMe-D, and MATα1-D cells. Results are shown as mean% of DMSO control ± SEM, $^{*}P < 0.05$, $^{**}P < 0.01$ vs. control. **D** Effects of varying concentrations BV02 treatments on migration of OKER, SAMe-D, and MATα1-D cells. Quantitative values are summarized in the graphs, expressed as mean% of DMSO control ± SEM from three experiments done in duplicates, $^{***}P < 0.001$, $^{****}P < 0.0001$ vs. control. **E** Effect of 5 μM BV02 treatments on invasion of OKER, SAMe-D, and MATα1-D cells. Quantitative values are summarized below the invasion images, expressed as mean% of total cells invaded ± SEM from three experiments done in duplicates, $^{*}P < 0.05$ vs. DMSO. **F**–**H** BrdU, migration, and invasion assays were done in OKER, SAMe-D, and MATα1-D cells after treatment with Ywhaz siRNA for 24 h first. Results are shown as mean% of scramble siRNA control (SC) ± SEM from three independent experiments done in duplicates, $^{**}P < 0.01$, $^{***}P < 0.001$, $^{****}P < 0.0001$ vs. SC.

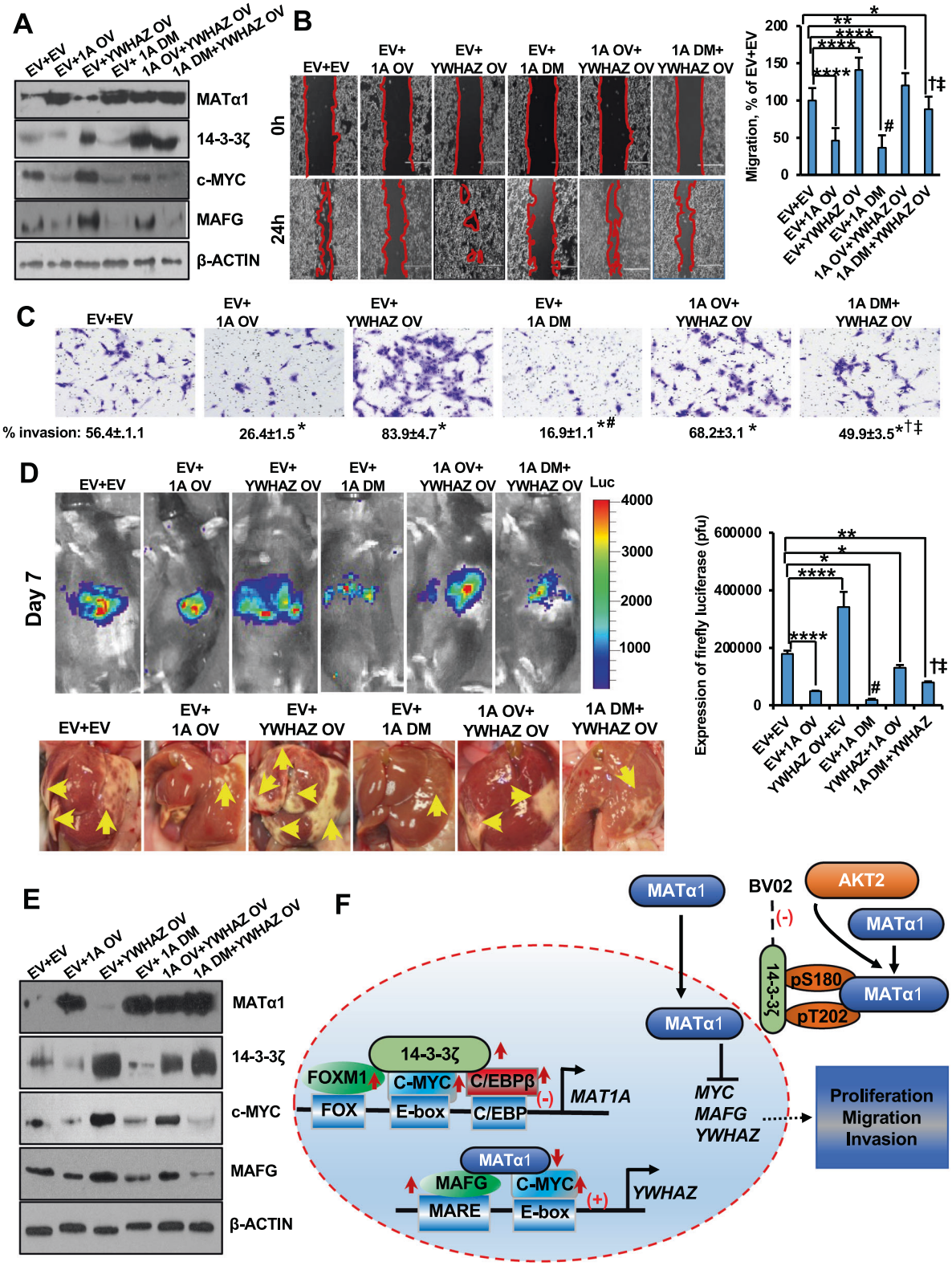

responsible for catalyzing the first and rate-limiting step of the hepatic urea cycle, which is critical for the removal of excess nitrogen [23]. CPS1 expression is lower in HCC and low expression correlates with shorter survival [23]. One possible explanation is that reduced urea cycle activity directs nitrogen to carbamoyl-phosphate-synthetase 2, aspartate transcarbamoylase, and dihydroorotase, which is often induced in HCC, to increases pyrimidine synthesis [23]. The finding that CPS1 is the top interacting protein of MATα1 suggests CPS1 might be regulated by methylation within the mitochondria, since MATα1 is also localized in the mitochondria in hepatocytes [17]. Downregulation of CPS1 in HCC has been attributed in part to promoter

Fig. 8 YWHAZ enhances cell migration, invasion, and tumor growth in part by keeping MATα1 out of the nucleus. A MzChA-1 cells were transfected with EV, MAT1A overexpression (1A OV), YWHAZ OV, MAT1A S180A and T202A double mutant (1A DM), alone or combined for 24 h. Western blotting effects on c-MYC and MAFG protein levels. **B** Representative migration images of MzChA-1 cells after the same treatments. Quantitative values are summarized in the graph. Results are mean% of EV + EV ± SEM from three experiments done in duplicates, $^{*}P < 0.05$, $^{**}P < 0.01$, $^{****}P < 0.0001$ vs. EV + EV; $^{\#}P < 0.05$ vs. EV + 1A OV; $^{\dagger}P < 0.05$ vs. EV + YWHAZ; $^{\ddagger}P < 0.05$ vs. 1A OV + YWHAZ. **C** Representative invasion images of HepG2 cells after the same treatments as in (**A**) are shown. Quantitative values are summarized below the images. Results are mean% of total cells invaded ± SEM from three experiments done in duplicates, $^{*}P < 0.05$ vs. EV + EV; $^{\#}P < 0.05$ vs. EV + 1A OV; $^{\dagger}P < 0.05$ vs. EV + YWHAZ OV; $^{\ddagger}P < 0.05$ vs. 1 A OV + YWHAZ. **D** Representative images of IVIS luciferase results in C57BL/6J mice ($n = 8$ per group) at day 7 following the metastatic HCC protocol described in Methods using MATα1-D cells. Representative pictures of metastatic liver cancers from these mice are shown below. Quantitative signals from the IVIS luciferase images are summarized in the graph below. $^{*}P < 0.05$, $^{**}P < 0.01$, $^{****}P < 0.0001$ vs. EV + EV; $^{\#}P < 0.05$ vs. EV + 1A OV; $^{\dagger}P < 0.05$ vs. EV + YWHAZ OV; $^{\ddagger}P < 0.05$ vs. 1A OV + YWHAZ. **E** Protein levels of MATα1, 14-3-3ζ, MAFG, and c-MYC from the above liver tumor tissues. (**F**) The schematic diagram shows a novel crosstalk between MAT1A and YWHAZ in liver cancers, where increased AKT2 activity phosphorylates MATα1 at S180 and T202, leading to increased binding by 14-3-3ζ that keeps MATα1 out of the nucleus and blocks its tumor suppressive effects. MAT1A and YWHAZ also exert a negative reciprocal regulation against each other at the transcriptional level. 14-3-3ζ negatively regulates *MAT1A* promoter via FOXM1, C/EBPβ, and c-MYC, all repressors of the *MAT1A* promoter, by increasing their expression, interacting with these transcription factors, and enhancing their binding to their respective *cis*-acting elements; whereas MATα1 negatively regulates *YHWAZ* transcription by suppressing c-MYC and MAFG expression and their binding to the MARE and E-box enhancer elements of the *YWHAZ* promoter. Interrupting interaction between 14-3-3ζ and MATα1 by either BV02 or mutating the two phosphorylation sites on MATα1 raises MATα1 nuclear content to exert liver cancer suppressive function, such as repressing oncogenic signaling of c-MYC, MAFG, and 14-3-3ζ.

hypermethylation [24]. Whether CPS1 activity is regulated by methylation is unknown, and whether mitochondrial MATα1 is dysregulated in HCC is also unknown. These are topics worthy of further investigation.

Since MATα1 must be phosphorylated in order to interact with 14-3-3ζ, we next investigated the responsible kinase(s). AKT2 appeared high on the prediction websites and is the only AKT that is hyperactive in HCC and CCA. AKT2 has been shown to be induced in 38% of HCC but more importantly, it is an independent prognostic indicator in HCC, whereas AKT1 was not [25]. In a mouse model of hepatic steatosis with carcinogenesis, ablation of AKT2 prevented both steatosis and tumorigenesis [26]. AKTs exert different effects on immune cells and the tumor microenvironment. A review of AKT family and strategies in targeting them in HCC treatment was recently published [27]. Not as much is known about AKT2 in CCA, although AKT2 was reported to be important in CCA growth in vitro [28]. We confirmed that AKT2 was able to phosphorylate MATα1 and knocking down AKT2 lowered the interaction between MATα1 and 14-3-3ζ. However, unexpectedly we found AKT2 knockdown raised the protein level of MATα1 by inhibiting MATα1 proteasomal degradation. How AKT2 regulates proteasomal activity will require further investigation.

In addition to interacting directly with each other, MATα1 and 14-3-3ζ also exert a complex reciprocal negative regulation against each other at the transcription level. Interestingly, 14-3-3ζ exerts its effect on the *MAT1A* promoter by interacting with FOXM1, c-MYC, and C/EBPβ and enhancing their binding to their respective elements in the *MAT1A* promoter. This explains why BV02, an inhibitor of 14-3-3 protein-protein interactions, was able to also lower the binding of FOXM1, c-MYC, and C/EBPβ to their respective elements and raise the *MAT1A* promoter activity. Indeed, 14-3-3ζ is highly expressed in the nuclei of HCC and has been reported to act as a transcription co-factor [29]. To the best of our knowledge 14-3-3ζ has not been reported to interact or influence the DNA binding activity of FOXM1, c-MYC, and C/EBPβ.

Another mechanism for 14-3-3ζ to suppress MAT1A expression is by inducing the expression of transcription factors that inhibit *MAT1A* promoter activity. For instance, 14-3-3ζ induces FOXM1 expression in breast cancer [30]. We also found 14-3-3ζ induces the expression of c-MYC and MAFG, both of which suppress MAT1A expression [2, 7]. Similarly, 14-3-3ζ induces all of the isoforms of C/EBPβ. Since the antibody we used recognizes all three isoforms on ChIP, we are not able to differentiate which isoform(s) are involved in repressing *MAT1A* promoter.

We also identified c-MYC and MAFG as direct inducers of *YWHAZ* transcription in liver cancer cells. We found MAFG, c-MYC and MATα1 interact at MARE and E-box elements of the *YWHAZ* promoter, with the first two acting as co-activators but MATα1 acting as a co-repressor. As far as we know, these are new mechanisms of *YWHAZ* transcriptional regulation. Previously c-MYC was shown to positively regulate YWHAZ expression by suppressing miR-451 in acute myeloid leukemia cells [31]. The question of whether MATα1 is acting as a bona fide transcription co-factor or is suppressing via epigenetics was examined comparing WT to the MAT1A catalytic mutant. Since the catalytic mutant failed to suppress YWHAZ expression, one possible mechanism is via epigenetics (e.g. DNA hypermethylation or H3K27 trimethylation). However, inhibiting DNA methylation or H3K27 trimethylation did not prevent MAT1A overexpression from lowering *YWHAZ* mRNA levels. Another possibility is that only polymeric MATα1 can interact with these transcription factors since the catalytic mutant cannot polymerize [2]. The finding that only WT MATα1 but not the catalytic mutant was able to interact with MAFG and c-MYC on Seq-ChIP supports the second possibility.

To address the importance of 14-3-3ζ interaction with MATα1 in the oncogenic activity of 14-3-3ζ, we compared the effects of co-overexpressing YWHAZ with either wild type or double mutant MAT1A (which can't interact with 14-3-3ζ) on cancer growth in vitro and in vivo using a metastatic HCC model in wild type immune competent mice. We found the double mutant MAT1A was best in reducing tumor growth and metastasis even when combined with YWHAZ overexpression. Taken together, these results suggest in liver cancer a key oncogenic mechanism for 14-3-3ζ is to suppress MAT1A expression and to keep MATα1 out of the nucleus. Supporting this notion is the finding that BV02 had no effect in HCC cells that did not express MAT1A. Since MAT1A is mainly expressed in hepatocytes and cholangiocytes, this mechanism may only be applicable in HCC and CCA.

In summary, we have unveiled a complex crosstalk between YWHAZ and MAT1A in HCC and CCA. They negatively regulate each other's gene transcription by influencing the expression and binding activity of multiple transcription factors. We also provide evidence that MATα1 is a novel substrate of 14-3-3ζ and identified AKT2, hyperactive in liver cancer, could phosphorylate MATα1 to enhance its interaction with 14-3-3ζ. The consequence of this interaction is to keep MATα1 out of the nucleus so that it is unable to suppress the expression of multiple oncogenes. Disrupting the interaction between MATα1 and 14-3-3ζ may be an attractive strategy to treat liver cancer. Figure 8F is a schematic summary of the key findings.

REFERENCES

1. Lu SC, Mato JM. S-adenosylmethionine in liver health, injury, and cancer. Physiological Rev. 2012;92:1515–42.
2. Yang H, Liu T, Wang J, Li TW, Fan W, Peng H, et al. Deregulated methionine adenosyltransferase α1, c-Myc, and Maf proteins together promote cholangiocarcinoma growth in mice and humans. Hepatology 2016;64:439–55.
3. Li Y, Lu L, Tu J, Zhang J, Xiong T, Fan W, et al. Reciprocal regulation between forkhead box M1/NF-kB and methionine adenosyltransferase 1A drives liver cancer. Hepatology 2020;72:1682–1700.
4. Torres L, Avila MA, Carretero MV, Latasa MU, Caballeria J, López-Rodas G, et al. Liver-specific methionine adenosyltransferase MAT1A gene expression is associated with a specific pattern of promoter methylation and histone acetylation: implications for MAT1A silencing during transformation. FASEB J. 2000;14:95–102.
5. Tomasi ML, Li TW, Li M, Mato JM, Lu SC. Inhibition of human methionine adenosyltransferase 1A transcription by coding region methylation. J Cell Physiol. 2012;227:1583–91.
6. Vázquez–Chantada M, Fernández–Ramos D, Embade N, Martínez–Lopez N, Varela–Rey M, Woodhoo A, et al. HuR/Methyl-HuR and AUF1 regulate the MAT expressed during liver proliferation, differentiation, and carcinogenesis. Gastroenterology 2010;138:1943–53.
7. Liu T, Yang H, Fan W, Tu J, Li TWH, Wang J, et al. Mechanisms of MAFG dysregulation in cholestatic liver injury and development of liver cancer. Gastroenterology 2018;155:557–71.
8. Murray B, Barbier-Torres L, Fan W, Mato JM, Lu SC. Methionine adenosyltransferases in liver cancer. World J Gastro. 2019;25:4300–19.
9. Yang H, Cho ME, Li TWH, Peng H, Ko KS, Mato JM, et al. MicroRNAs regulate methionine adenosyltransferase 1A expression in hepatocellular carcinoma. J Clin Invest. 2013;123:285–98.
10. Fan W, Yang H, Liu T, Wang J, Li TWH, Mavila N, et al. Prohibitin 1 suppresses liver cancer tumorigenesis in mice and human hepatocellular and cholangiocarcinoma cells. Hepatology 2017;65:1249–66.
11. Yang H, Li TWH, Peng J, Tang X, Ko KS, Xia M, et al. A mouse model of cholestasis-associated cholangiocarcinoma and transcription factors involved in progression. Gastroenterology 2011;141:378–88.
12. Xia Q, Li Z, Zheng J, Zhang X, Di Y, Ding J, et al. Identification of novel biomarkers for hepatocellular carcinoma using transcriptome analysis. J Cell Physiol. 2019;234:4851–63.
13. Johnson C, Crowther S, Stafford MJ, Campbell DG, Toth R, MacKintosh C. Bioinformatic and experimental survey of 14-3-3-binding sites. Biochem J. 2010;427:69–78.
14. Root A, Beizaei A, Ebhardt HA. Structure-based assessment and network analysis of targeting 14-3-3 proteins in prostate cancer. Mol Cancer. 2018;17:156.
15. Reytor E, Pérez-Miguelsanz J, Alvarez L, Pérez-Sala D, Pajares MA. Conformational signals in the C-terminal domain of methionine adenosyltransferase I/III determine its nucleocytoplasmic distribution. FASEB J. 2009;23:3347–60.
16. Pérez C, Pérez-Zúñiga FJ, Garrido F, Reytor E, Portillo F, Pajares MA. The oncogene PDRG1 is an interaction target of methionine adenosyltransferases. PLoS One. 2016;11:e0161672.
17. Murray B, Peng H, Barbier-Torres L, Robinson AE, Li TWH, Fan W, et al. Methionine adenosyltransferase α1 is targeted to the mitochondrial matrix and interacts with cytochrome P450 2E1 to lower its expression. Hepatology 2019;70:2018–34.
18. Frau M, Feo F, Pascale RM. Pleiotropic effects of methionine adenosyltransferases deregulation as determinants of liver cancer progression and prognosis. J Hepatol. 2013;59:830–41.
19. Muslin AJ, Tanner JW, Allen PM, Shaw AS. Interaction of 14-3-3 with signaling proteins is mediated by the recognition of phosphoserine. Cell 1996;84:889–97.
20. Yaffe MB, Rittinger K, Volinia S, Caron PR, Aitken A, Leffers H, et al. The structural basis for 14-3-3:phosphopeptide binding specificity. Cell 1997;91:961–71.
21. Graves PR, Lovly CM, Uy GL, Piwnica-Worms H. Localization of human Cdc25C is regulated both by nuclear export and 14-3-3 protein binding. Oncogene 2001;20:1839–51.
22. Tang Y, Lv P, Sun Z, Han L, Luo B, Zhou W. 14-3-3ζ up-regulates hypoxia-inducible factor-1α in hepatocellular carcinoma via activation of PI3K/Akt/NF-κB signal transduction pathway. Int J Clin Exp Path. 2015;8:15845–53.
23. Ridder DA, Schindeldecker M, Weimann A, Berndt K, Urbansky L, Witzel HR, et al. Key enzymes in pyrimidine synthesis, CAD and CPS1, predict prognosis in hepatocellular carcinoma. Cancers 2021;13:744.
24. Liu H, Dong H, Robertson K, Liu C. DNA methylation suppresses expression of the urea cycle enzyme carbamoyl phosphate synthetase 1 (cps1) in human hepatocellular carcinoma. Am J Pathol. 2011;178:652–61.
25. Xu X, Sakon M, Nagano H, Hiraoka N, Yamamoto H, Hayashi N, et al. Akt2 expression correlates with prognosis of human hepatocellular carcinoma. Oncol Rep. 2004;11:25–32.
26. Wang C, Che L, Hu J, Zhang S, Jiang L, Latte G, et al. Activated mutant forms of PIK3CA cooperate with RasV12 or c-Met to induce liver tumour formation in mice via AKT2/mTORC1 cascade. Liver Int. 2016;36:1176–86.
27. Mroweh M, Roth G, Decaens T, Marche PN, Lerat H, Jílková ZM. Targeting Akt in hepatocellular carcinoma and its tumor microenvironment. Int J Mol Sci 2021;22:1794.
28. Ewald F, Grabinski N, Grottke A, Windhorst S, Nörz D, Carstensen L, et al. Combined targeting of AKT and mTOR using MK-2206 and RAD001 is synergistic in the treatment of cholangiocarcinoma. Int J Cancer 2013;133:2065–76.
29. Yu M, Guo HX, Hui C, Wang XH, Li CY, Zhan YQ, et al. 14-3-3ζ interacts with hepatocyte nuclear factor 1α and enhances its DNA binding and transcriptional activation. Biochimica et Biophysica Acta. 2013;1829:970–79.
30. Bergamaschi A, Christensen BL, Katzenellenbogen BS. Reversal of endocrine resistance in breast cancer: interrelationships among 14-3-3ζ, FOXM1, and a gene signature associated with mitosis. Breast Cancer Res. 2011;13:R70.
31. Su R, Gong JN, Chen MT, Song L, Shen C, Zhang XH, et al. c-Myc suppresses miR-451⊣YWTAZ/AKT axis via recruiting HDAC3 in acute myeloid leukemia. Oncotarget 2016;7:77430–43.
32. Peng H, Dara L, Li TWH, Zheng Y, Yang HP, Tomasi ML, et al. MAT2B-GIT1 interplay activates MEK1/ERK 1 and 2 to induce growth in human liver and colon cancer. Hepatology 2013;57:2299–313.

ACKNOWLEDGEMENTS

This work was supported by NIH grants DK123763 (HP Yang, JM Mato and SC Lu), P01CA233452 (HP Yang, E Seki, ML Tomasi, N Bhowmick, and SC Lu), Natural Science Foundation General Program of Hunan Province NO.2018JJ2664 (T Liu), and Plan Nacional of I+D SAF2017-88041-R (JM Mato). The funders had no role in study design, data collection and analysis, decision to publish, or preparation of the manuscript.

AUTHOR CONTRIBUTIONS

LL and JZ, data collection, analysis and interpretation, figure preparation and drafting of the manuscript; WF and YL, data collection, analysis, interpretation and figure preparation; JW, TWHL and LBT, cell culture, analysis and interpretation; JMM, ES, and NAB, critical reading, editing of manuscript and intellectual content. TL, provided human biospecimens; MM and MLT, technical assistance; HY, data collection, analysis, interpretation, figure preparation and drafting of the manuscript. SCL, study concept and design, data interpretation, edited the manuscript, obtained funding and provided overall study supervision.

COMPETING INTERESTS

The authors declare no competing interests.

ADDITIONAL INFORMATION

Supplementary information The online version contains supplementary material available at https://doi.org/10.1038/s41388-021-01980-6.

Correspondence and requests for materials should be addressed to H.Y. or S.C.L.

Reprints and permission information is available at http://www.nature.com/reprints

Publisher's note Springer Nature remains neutral with regard to jurisdictional claims in published maps and institutional affiliations.